SUPPLEMENTAL METERIAL

Calculation of the action potential duration (APD) map

In the reduced calcium ($[Ca]_i$) -APD system, where intracellular sodium ($[Na]_i$) is clamped (Fig. 4B), we constructed APD maps to illustrate the nonlinearity in the system for bistability. Denote the APD of the i^{th} AP during periodic pacing by APD_i and its associated diastolic interval (DI) by DI_i. The APD map, i.e. the one-dimensional finite difference equation $APD_n = f(APD_{n-1})$ can be constructed from the APD restitution (or APD recovery curve), as shown by Yeti et al (1). The APD restitution assumes that at arbitrary pacing cycle length (PCL), APD is determined only by its preceding DI (Eq. 1),

$$APD_n = g(DI_{n-1}) \qquad \text{(Eq. 1)}$$

By definition, $PCL = APD + DI$, thus,

$$APD_{n-1} = PCL - DI_{n-1}, \qquad \text{(Eq. 2)}$$

Substituting Eq. 2 into Eq. 1, one has

$$APD_n = g(PCL - APD_{n-1}) = f(APD_{n-1}) \qquad \text{(Eq. 3)}$$

To obtain the steady-state APD restitution, we paced the cell at an arbitrary DI_{n-1} till APD_n reaches its steady state. Then by varying DI_{n-1}, we determined the steady-state APD restitution (*g*). At a specific PCL (1.8 s in this study), Eq. 3 gives the APD map (*f*).

Since V is coupled to $[Ca]_i$ (Fig. 3B), a more accurate map of the system would require $[Ca]_i$ also. Although a different $[Ca]_i$ level shifted the APD map, it did not change the solution qualitatively (Fig. S3A).

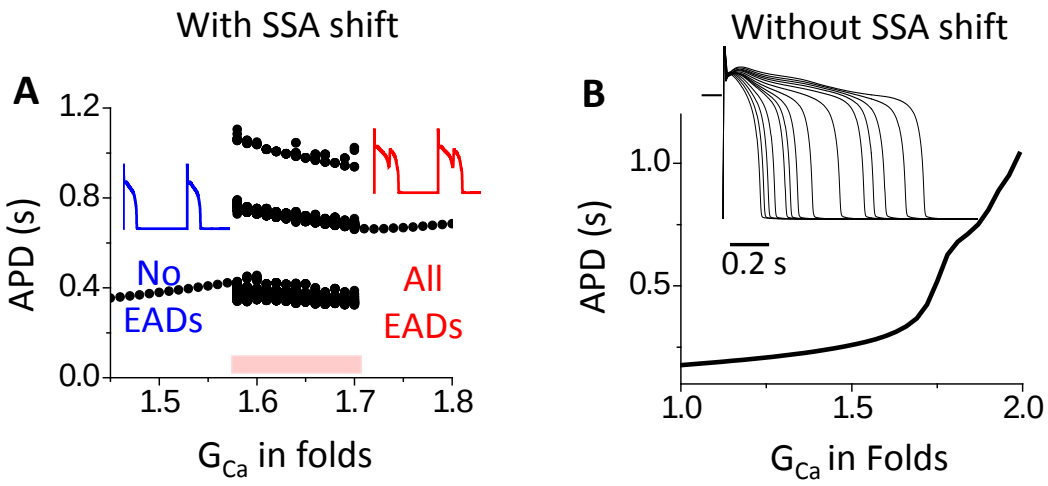

Fig. S1. Dependence of APD on G_{Ca}. A. With a -5 mV shift of the steady-state activation (SSA) gate of I_{CaL}, increasing G_{Ca} (> 1.57 folds) causes intermittent EADs within a range (red bar), after which EADs persist. **B**. Without the shift in I_{CaL} activation, increasing G_{Ca} alone prolongs APD but dos not induce EAD (inset). To avoid spontaneous Ca release at long AP, EC_{50} of the SR Ca release was increased by 50%.

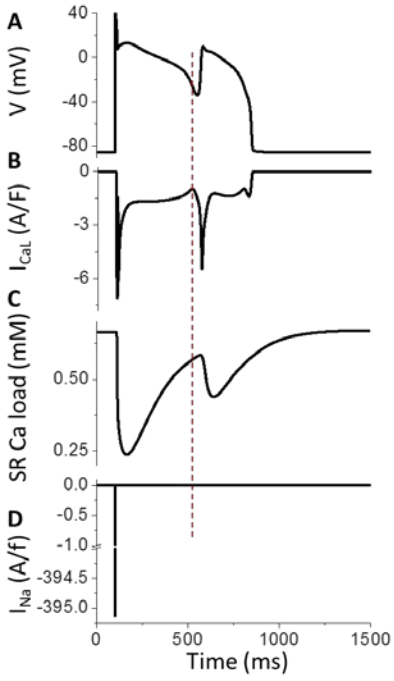

Fig. S2. EAD is due to I_{CaL} reactivation. Voltage (**A**), I_{CaL}(**B**), SR Ca (**C**) and I_{Na} (**D**) are aligned to show that I_{CaL} reactivation precedes EAD take off and the secondary Ca release (dashed line). There is no I_{Na} reactivation underlying the EAD (D).

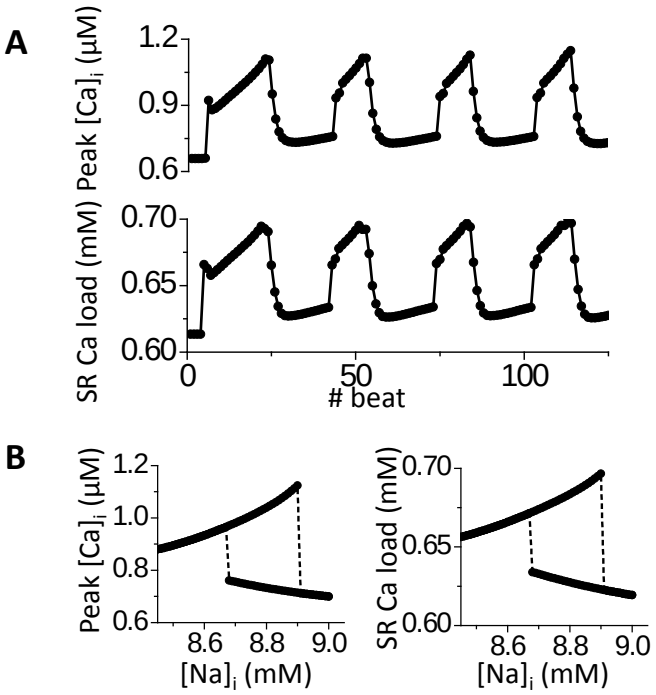

Fig. S3. Hysteresis and bistability in peak $[Ca]_i$ and SR Ca load. A. Both peak $[Ca]_i$ (top) and SR Ca load (bottom) corresponding to the APDs in Fig. 2 show similar oscillation to the diastolic $[Ca]_i$ (Fig. 2A middle). **B.** Bistability exists in both peak $[Ca]_i$ (left) and SR Ca load (right).

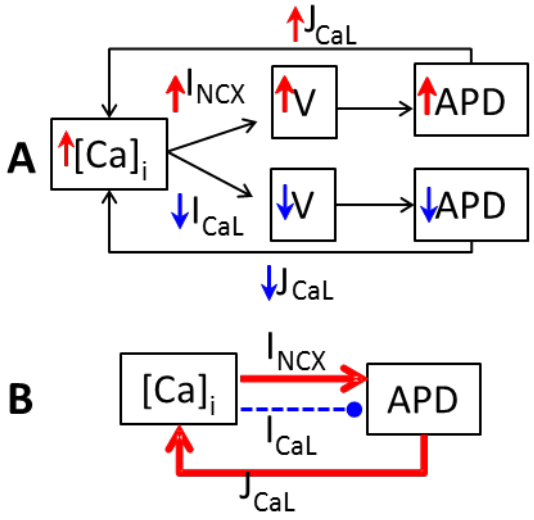

Fig. S4. Schematic of the bi-directional coupling between $[Ca]_i$ and membrane V in cardiac myocytes. A. $[Ca]_i$ regulates membrane V and thus APD through I_{CaL} and I_{NCX}; APD in turn modulates $[Ca]_i$ via Ca fluxes, J_{Ca}. B. Simplified $[Ca]_i$-APD feedback schematic from A. Red solid – activation; blue dashed – suppression.

Bistability does not occur in the model with negative $[Ca]_i$-APD feedback

To further test the hypothesis that a strong positive $[Ca]_i$-APD feedback is required for bistable early afterdepolarization (EAD)-no EAD pattern, we investigated whether bistability can occur in EAD enabling models with negative $[Ca]_i$-APD feedback. We set the maximum conductance of the Na-Ca exchanger current (G_{NCX}) to 0 to ensure a negative $[Ca]_i$-APD feedback (Fig. 4Bb), while permitting Ca extrusion via I_{NCX} (J_{NCX}). In this condition (reduced inward current) we additionally decreased potassium (K) currents (see figure legends) to achieve AP prolongation, I_{CaL} reactivation and EAD formation (Fig. S3B) as in control (Fig. S1A). We investigated two cases: 1) periodic 1 EAD (Fig. S5B cyan, AP #2), and 2) irregular EADs (Figs. S5B pink (AP #3) and C). In both cases, APD decreases with increasing $[Na]_i$, showing no bistability (Fig. S5D cyan and pink correspondingly). APD maps of the periodic 1 EAD reveal only one branch (the EAD branch) that forms one stable fixed point (Fig. S5D cyan). In the irregular EADs, nonlinearity exists and the APD map shows two branches (Fig. S5D pink). However, only one intersection is possible (Fig. S5D pink), as APD_n negatively correlates to APD_{n-1} due to the negative $[Ca]_i$-APD feedback. This confirms that bistability requires a positive $[Ca]_i$-APD feedback, which occurs when I_{NCX} dominates over I_{CaL}.

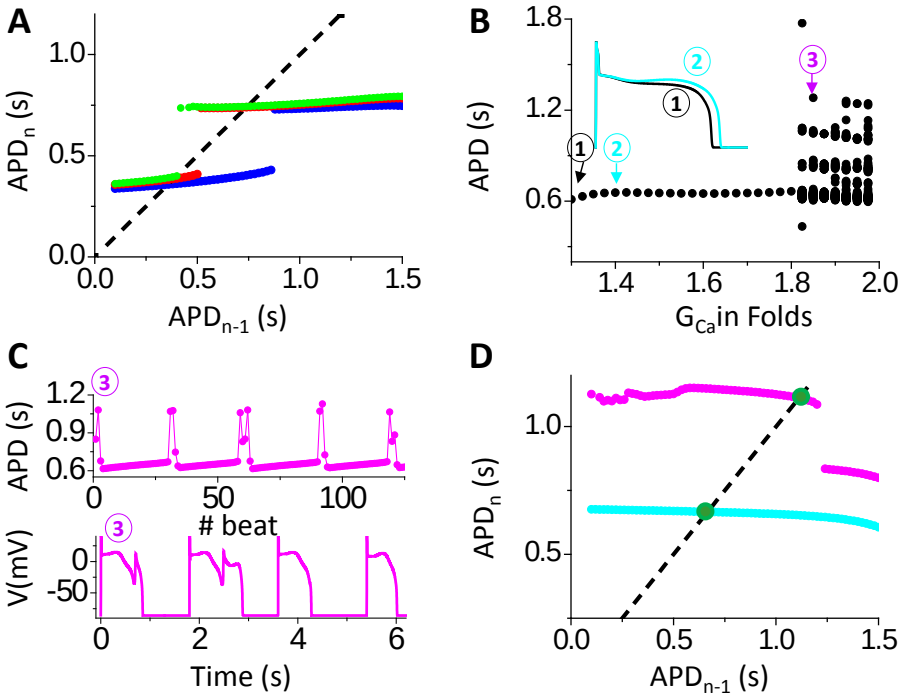

Fig. S5. Weakening the $[Ca]_i$-APD positive feedback abolishes bistability. A. APD maps are shifted when $[Ca]_i$ is varied (green, 0.196 μM; red, 0.183 μM; and blue, 0.187 μM), but do not change qualitatively. **B.** Dependence of APD on G_{Ca} when G_{NCX}=0 (both G_{Kr} and $G_{to,s}$ are decreased to 5% in this analysis). As G_{Ca} value increases to 1.4-fold, APD changes smoothly from no EAD (#1 black) to periodic 1 (low-amplitude) EAD occurs (#2 cyan, inset). Irregular EADs occur for larger G_{Ca} (#3, pink). **C.** APD trace (top) and AP profiles of the first 4 beats (bottom) from #3 in panel B. **D.** APD maps for periodic 1 EAD and irregular EADs (seen in panel B and Fig. 4D). The black dotted line is the identity line. Only one intersection (green dot) is possible in both.

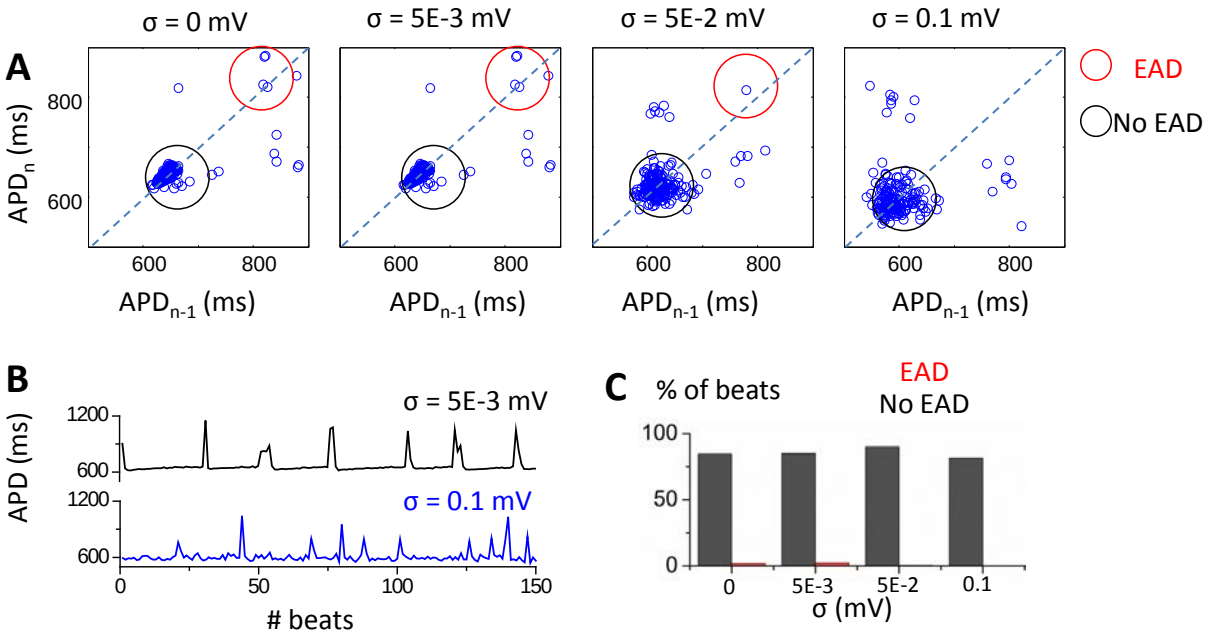

Fig. S6. APD Poincaré plots in the model without bistable EAD switches (G_{NCX}=0). A. Only one cluster (the no EAD cluster) exists, especially with noise. **B.** APD time series at the low and high levels of noise (σ=0.005 mV (black) vs. σ=0.1 mV (blue)). **C.** Fraction of total beats in EAD (red) and no EAD cluster (black) for various noise levels.

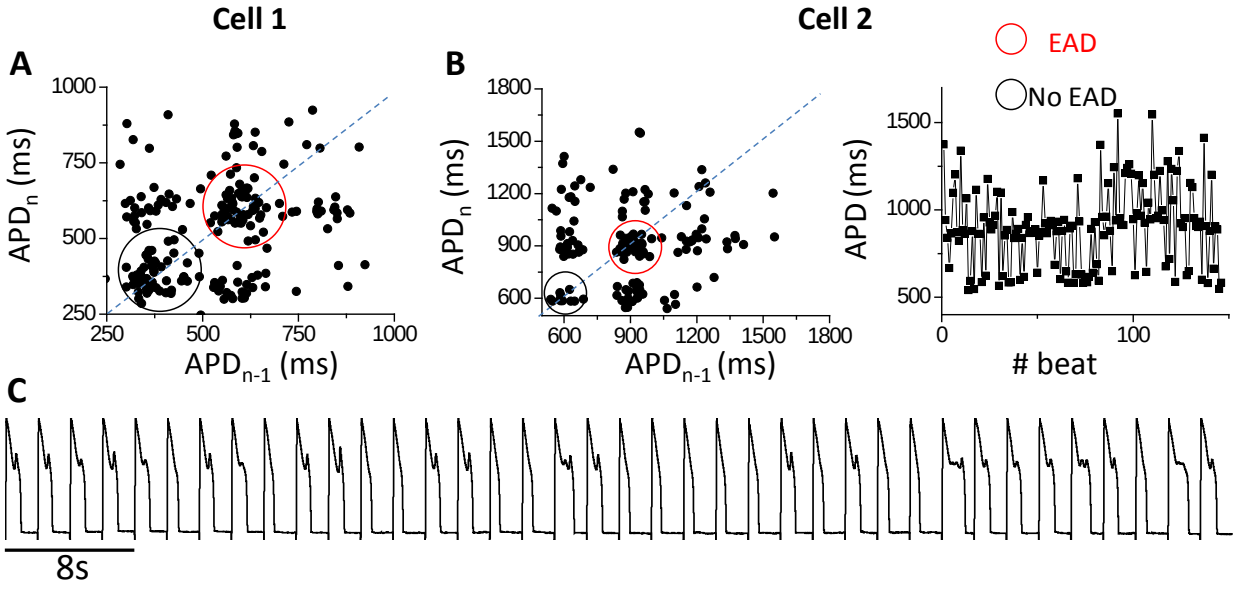

Fig. S7. Coexistence of EAD and no EAD clusters in experiments. A. APD Poincaré plot of Fig. 6Ba is redrawn to include the full axis range. Dotted line is the identity line. Red and black circles indicate the clusters with and without EADs respectively. **B.** APD Poincaré plot from the cell in Fig. 6Bb is redrawn to include the full axis range (left), along with the corresponding APD sequence (right). **C.** A sample of AP trace from the experiment in panel B.

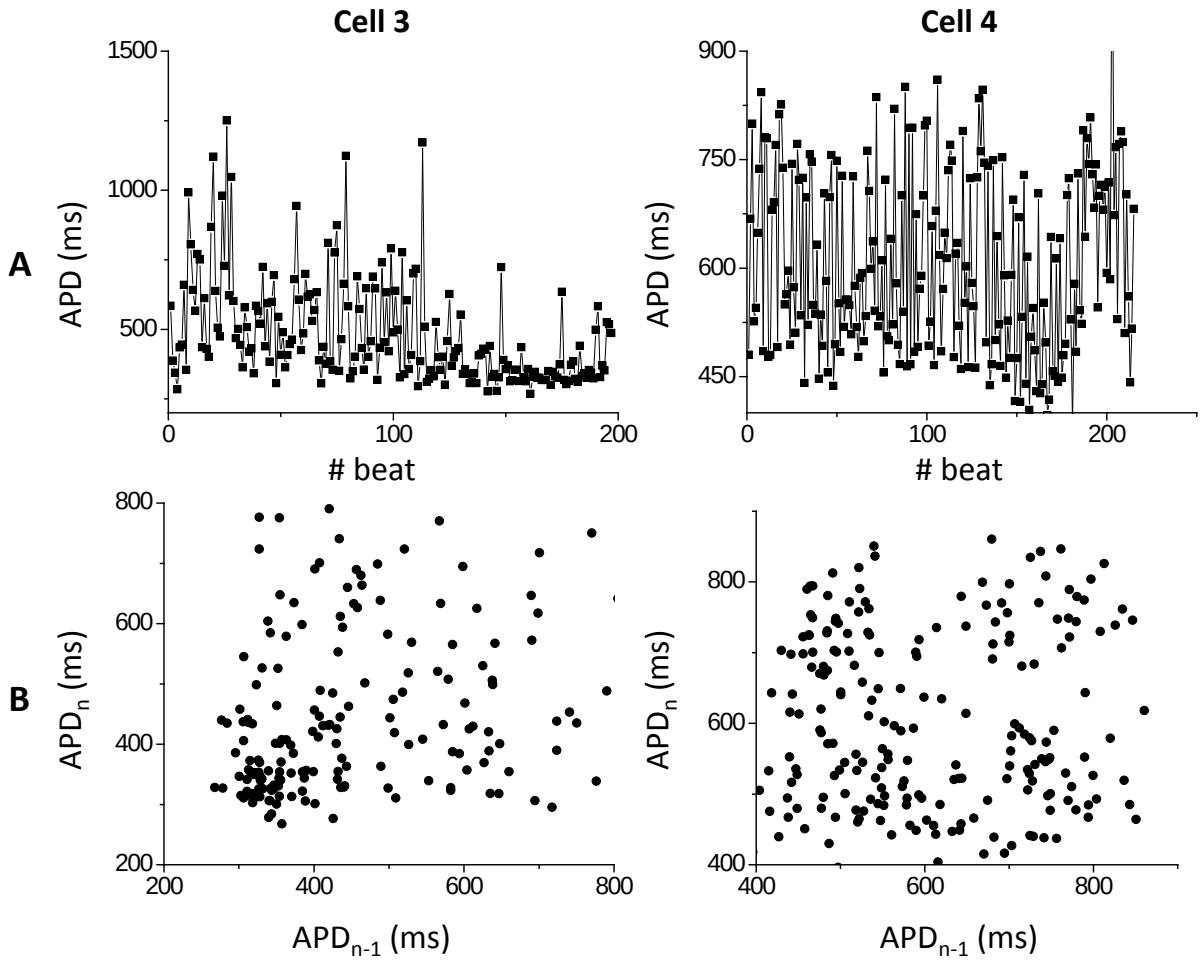

Fig. S8. Recordings from two cells that do not show clear coexistence of EAD and no EAD clusters. A. APD sequences. **B.** APD Poincaré plots.

References

1. Yehia AR, Jeandupeux D, Alonso F, & Guevara MR (1999) Hysteresis and bistability in the direct transition from 1:1 to 2:1 rhythm in periodically driven single ventricular cells. *Chaos* 9(4):916-931.